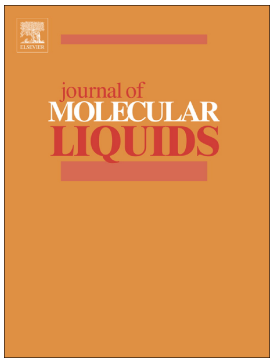

A double signal optical probe composed of carbon quantum dots and Au@Ag nanoparticles grown in situ for the high sensitivity detection of ellagic acid

Xiu Qin, Chunling Yuan, Rui Shi, Yilin Wang

PII: S0167-7322(20)35321-6

DOI: https://doi.org/10.1016/j.molliq.2020.114594

Reference: MOLLIQ 114594

To appear in: *Journal of Molecular Liquids*

Received date: 14 August 2020

Revised date: 10 October 2020

Accepted date: 14 October 2020

Please cite this article as: X. Qin, C. Yuan, R. Shi, et al., A double signal optical probe composed of carbon quantum dots and Au@Ag nanoparticles grown in situ for the high sensitivity detection of ellagic acid, *Journal of Molecular Liquids* (2020), https://doi.org/10.1016/j.molliq.2020.114594

A double signal optical probe composed of carbon quantum dots and Au@Ag nanoparticles grown in situ for the high sensitivity detection of ellagic acid

Xiu Qin, Chunling Yuan, Rui Shi, Yilin Wang*

(*School of Chemistry and Chemical Engineering, Guangxi Key Laboratory of Biorefinery, Guangxi University, Nanning 530004, China*)

Abstract: Carbon quantum dots (CQDs) were prepared from trifolium leaves via hydrothermal method, a fluorometric and colorimetric double signal probe based on CQDs-gold nanoparticles (AuNPs)-$AgNO_3$ system was constructed for the detection of ellagic acid (EA). In this system, Ag^+ ions were reduced by EA to Ag atoms, which deposited on the surfaces of AuNPs to form Au@AgNPs in situ, along with an obvious color change from pink to yellow. Simultaneously, the fluorescence of CQDs was quenched by Au@AgNPs attributing to inner filter effect (IFE). Under the optimal conditions, sensitive assay of EA was achieved, with the limit of detection (LOD) of 0.41 μM for fluorescence analysis and 0.22 μM for colorimetric assay. The changes of fluorescence and absorbance correlated well with EA concentration in the range of 0.50-25.0 μM. In addition, the double signal probe also exhibited high selectivity toward EA. The feasibility of the probe was confirmed in commercial cosmetics analysis with satisfactory results.

Keywords: Gold nanoparticles; Determination; Fluorescence; Colorimetry

1. Introduction

In recent years, with the development of nanoscience and nanotechnology, nanomaterials are widely used in various analytical methods [1,2]. Noble metal nanoparticles, such as gold nanoparticles (AuNPs) and silver nanoparticles (AgNPs), are favored in colorimetric analysis because of their surface plasmon resonance absorption (SPR)-related tunable optical properties [3,4]. For example, after aggregation, the SPR absorption peak of AuNPs and AgNPs shifts to a longer wavelength, accompanied by a significant color change of a solution. Because of its advantages of simplicity, rapidity and no need of expensive instrument, colorimetric method based on

*Corresponding author, E-mail address:theanalyst@163.com (Y. Wang); theanalyst@gxu.edu.cn (Y. Wang)

analyte-induced aggregation of AuNPs [5] and AgNPs [6] has been employed for detection of different substances such as terbuthylazine, dimethoate, and heavy metal ions. Besides, the growth or etching of AuNPs and AgNPs can also result in obvious color changes, which have been applied to assay of formaldehyde [7], glucose [8,9], alkaline phosphatase [10], pesticides [11], and so on. As an advanced nanomaterial, carbon quantum dots (CQDs) have been widely used in chemical analysis [12,13], fluorescence imaging [14-16] and catalysis [17-20] due to their advantages of simple preparation, no toxicity and good water solubility. The researches [21-23] demonstrated that CQDs fluorescence could be quenched by noble metal nanoparticles including AuNPs, AgNPs, and Au@AgNPs. A series of switches on fluorescence probes composed of CQDs and noble metal nanoparticles have been constructed for the detection of melamine [21], biothiols [22] and organophosphate pesticides [23]. In fact, AuNPs and AgNPs quench the fluorescence of CQDs, accompanied by their own color changes. Therefore, the above-mentioned probes have also been used for the assay of glucose [24], alkaline phosphatase [25], glutathione [26] and pesticides [27-29] by fluorescence and colorimetric methods.

Ellagic acid (EA) has a molecular structure comprising a planar biphenyl moiety bridged by two lactone rings and four hydrogen-bonding OH groups (Fig.1). As a kind of natural polyphenol antioxidant, EA widely exists in various fruits and nuts [30, 31], and its antioxidant effect has attracted much attention [32]. In addition, as a satisfactory whitening ingredient in cosmetics, EA can suppress melanin production by inhibiting tyrosinase activity [33]. A variety of analytical methods, such as UV-vis [34], resonance light scattering (RLS) [35,36], high performance liquid chromatography (HPLC) [37], capillary electrophoresis (CE) [38], voltammetry [31] and fluorimetry [39, 40], have been used for the determination of EA in various samples. Although these methods have the advantages of high sensitivity and good selectivity, they are all single signal response analysis. In this work, CQDs were prepared by hydrothermal treatment of trifolium leaves, and AuNPs were obtained by reduction of chloroauric acid with sodium citrate, a double signal probe composed of CQDs and Au@AgNPs grown in situ was designed for EA determination by fluorescence and colorimetric methods. As far as we know, there is no report on the determination of EA with CQDs- AuNPs-$AgNO_3$ system as double signal probe.

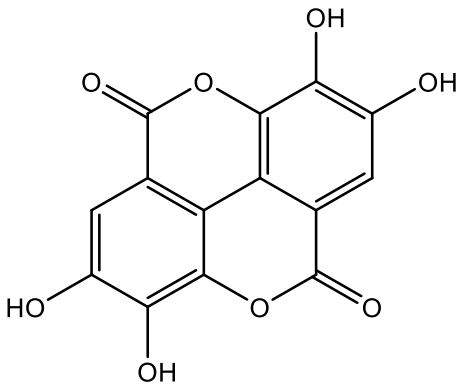

Fig.1. Structure of Ellagic acid (EA)

2. Experimental

2.1 Chemicals and apparatus

Chloroauric acid ($HAuCl_4$), Citric acid and Ellagic acid (EA) were obtained from McLean Biochemical Co., Ltd (Shanghai, China). Acetic acid glacial (CH_3COOH), Phosphoric acid (H_3PO_4), Boric acid (H_3BO_3), Sodium hydroxide (NaOH), Silver nitrate ($AgNO_3$), Ethyl alcohol, Glycerol, and Glycol were purchased from Guangdong Guanghua Sci-Tech Co., Ltd. Doubly deionized water (DDW) was utilized for preparing of all aqueous solutions.

The fluorescence spectra and UV-vis absorption spectra were achieved, respectively, with a RF-5301PC spectrophotometer (Shimadzu, Kyoto, Japan) and a UV-4802 (Unico, Shanghai, China). The morphology and size of CQDs and AuNPs were attained by transmission electron microscopy (TEM) (JEM 1200EX, Japan). FTIR spectra were recorded on a Nicolet iS50 FTIR spectrometer (Thermo Scientific Co., Ltd. Madison, WI, USA). The pH values of the solutions were measured with a PXSJ-216 pH meter (Shanghai Precision Science Instrument Co., Ltd., China). The measurement of zeta potential was carried out on a Brookhaven instrument (NanoBrook Omni, USA)

2.2 Preparation of CQDs and AuNPs

The CQDs were prepared by hydrothermal treatment of fresh Trifolium leaves. Briefly, 5.0 g of chopped Trifolium leaves was mixed with 30 mL of DDW, and then the mixture was transferred into a 75-mL Teflon-line autoclave and kept at 200°C for 10 h. After cooled to room temperature, the brown solution of upper layer was filtered with 0.22 μm membrane and then dialyzed (MWCO: 3500 Da) with DDW for 12 h. Finally, the solution containing CQDs was collected and stored in a

refrigerator at 4°C for further use.

The preparation of AuNPs was conducted according to the literature method [41], which was provided in Supplementary information.

2.3 Procedure for EA determination

The EA with different concentrations (5 - 250 μM, 200μL) were added to a series of 2.0-mL calibrated test tubes containing Britton-Robison (BR) buffer (1380 μL, pH 8.5), 200 μL of 2 mM $AgNO_3$, 20 μL of 5 nM AuNPs and 200 μL CQDs. After 6 min, the resulted mixtures were for fluorescence and UV-vis measurements, respectively. The fluorescence spectra of the mixture were recorded under excitation wavelength of 350 nm, and the excitation and emission slit widths were 5nm and 3nm, individually. UV-vis spectra were recorded in the range of 350-600 nm. All measurements were performed at room temperature. The concentration of EA was calculated based on the decreased fluorescence (ΔF) and increased absorbance (ΔA). In this work, ΔF is defined as (F - F_0), where F_0 and F are the fluorescence intensities of CQDs-AuNPs-$AgNO_3$ system at 405 nm in the absence and presence of EA, respectively, and $\Delta A = A - A_0$, where A_0 and A denote the absorbance at 413 nm in the absence and presence of EA, respectively.

3. Results and discussion

3.1 Choice of materials

Because of their unique optical properties, CQDs were used as fluorescence probes, Au@AgNPs as quencher and colorimetric probe in this study. Compared with traditional organic fluorescent dyes and inorganic semiconductor quantum dots, CQDs have the advantages of simple preparation, strong luminescence, high stability, no toxicity and good biocompatibility [42]. The excellent properties of CQDs make them ideal fluorescent probes for double signal analysis. Au@AgNPs have large molar extinction coefficient due to the surface plasmon absorption [43], which makes them widely used as fluorescence quenchers. Moreover, the absorption of Au@AgNPs is very sensitive to core-to-shell ratio and the distance between particles, which causes significant color changes. In a word, Au@AgNPs can be used as ideal absorbers to modulate the fluorescence of CQDs, and as colorimetric probes to achieve the colorimetric analysis in dual-mode assay.

3.2 Characterization of CQDs and AuNPs

TEM was used to characterize the morphology and particle sizes of CQDs and AuNPs. The

results in Fig. 2A confirm that the CQDs are uniformly spherical with a particle size ranging of 1.0-3.0 nm. The average diameter of the CQDs is estimated to be 2.0 nm, consistent with those in the literatures [26,44]. As shown in Fig. 2B, the AuNPs are spherical with good dispersion and a uniform particle size, and the average particle size is about 13 nm. The FTIR spectroscopy was used to characterize the functional groups on the surface of CQDs, as described in Fig. 2C. An obvious band at 3370 cm^{-1} is due to -OH group, and the peak at 3240 cm^{-1} corresponds to the characteristic vibration of -NH groups. The strong peak at 2930 cm^{-1} is assigned to the C-H stretching. Moreover, the characteristic bands at 1670 cm^{-1} and 1600 cm^{-1} indicate the presence of –C=O and –C=C stretching vibration, respectively. The absorption peak at 1110 cm^{-1} shows the presence of C-OH and peak at 807 cm^{-1} is due to the C-H bending vibrations. As depicted in Fig. 2D, the CQDs exhibit excitation wavelength-dependent emission properties. With the increase of excitation wavelength from 310 to 410 nm, emission peaks are red-shifted from 400 to 470 nm, and the emission intensity reaches a maximum when excited at 350 nm. According to the calculation method from literature [45], the CQDs exhibit a high fluorescence quantum yield (QY) of 23% with rhodamine 6G as a reference standard (QY = 95%), sufficient for various fluorescence sensing.

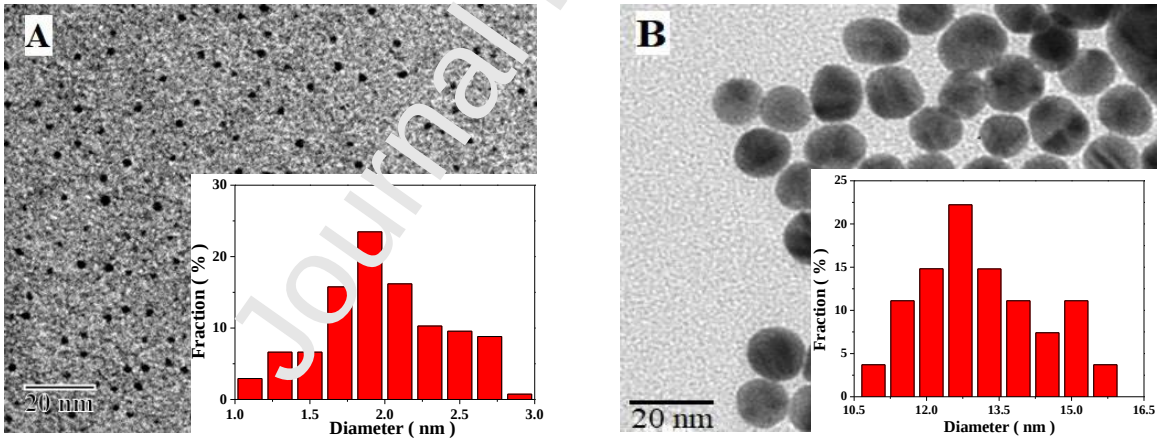

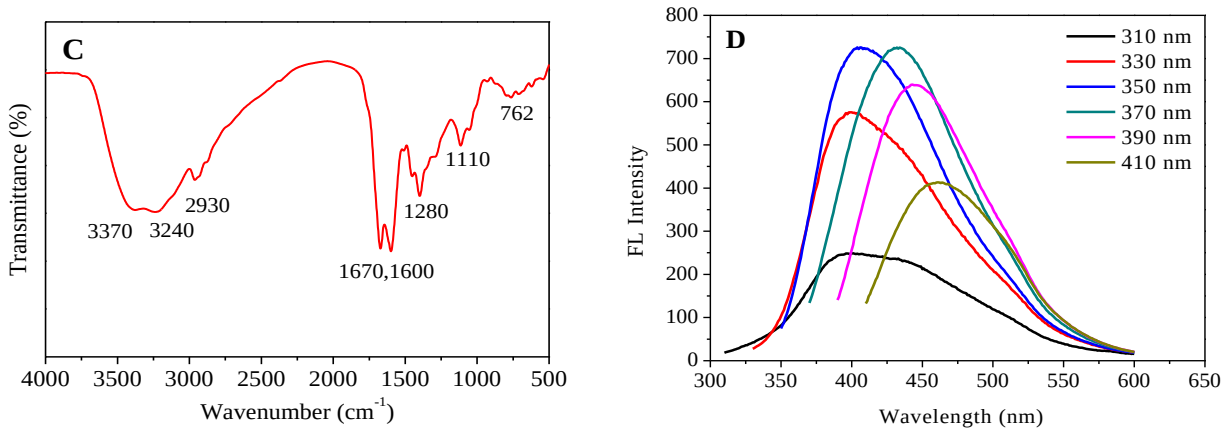

Fig.2. TEM images and size distributions of (A) CQDs and (B) AuNPs; (C) FTIR spectra of CQDs; (D) Excitation dependent fluorescence spectra of CQDs

3.3 Feasibility of double signal detection

As a phenolic antioxidant, EA can be oxidatively converted into the highly conjugated bis (ortho-quinone) [46]. Scheme 1 outlines the mechanism of double signal detection. EA reduces Ag^{+} to Ag^{0} which deposit on the surfaces of AuNPs to form Au@AgNPs, along with an obvious color change from pink to yellow. Simultaneously, the fluorescence of CQDs is efficiently quenched, attributing to inner filter effect (IFE) between CQDs and Au@AgNPs.

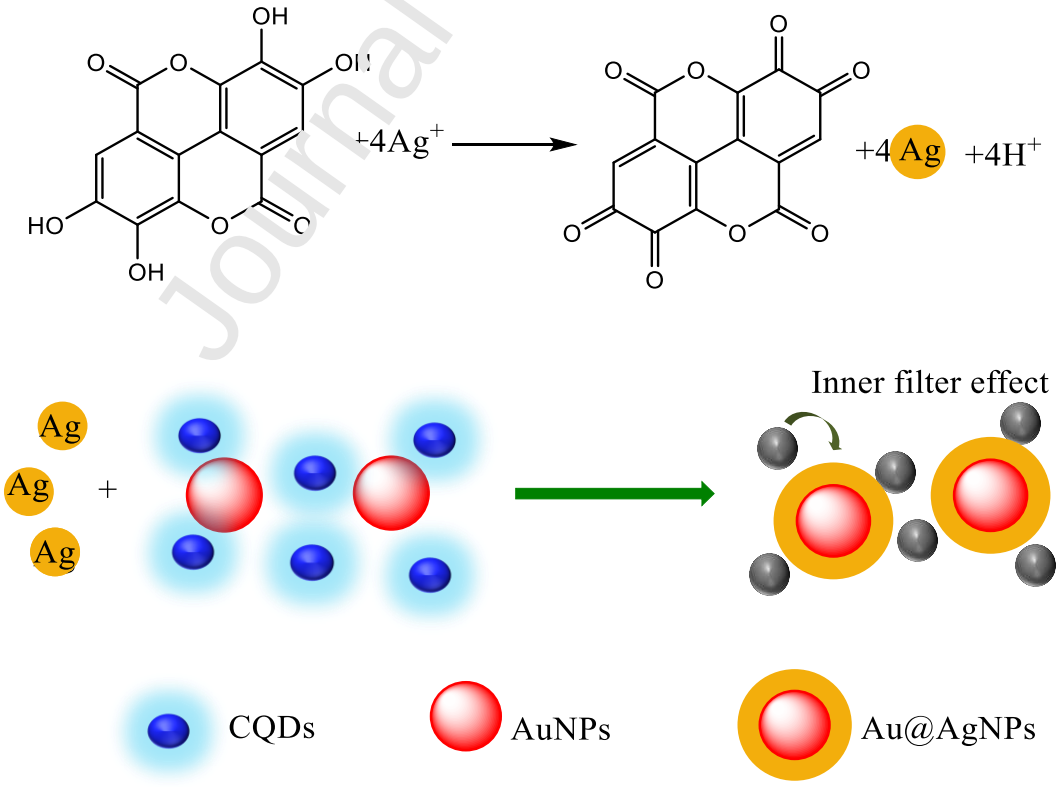

Scheme1. Schematic illustration of the mechanism of EA detection based on CQDs and Au@AgNPs.

TEM images, UV-Vis absorption and fluorescence spectra were used to investigated the feasibility of the method. Compared with the as-prepared AuNPs (Fig. 2B), a layer of shell can be clearly observed on the surfaces of AuNPs after adding Ag^+ ions and EA (Fig.S1). The surface plasmon resonance (SPR) absorption peak of AuNPs shifts from 520 nm (curve a in Fig.3A) to 410 nm (curve b in Fig.3A), along with an obvious color change from pink to yellow (inset in Fig.3A), which indirectly demonstrates the formation of a thin layer of Ag on the surface of AuNPs. As shown in Fig. 3B, excited by 350 nm wavelength light (curve a in Fig.3B), the emission peak of CQDs is located at 413 nm, and there is a large overlap between CQDs fluorescence spectra and Au@AgNPs absorption spectra (curves b and c in Fig.3B), suggesting that CQDs fluorescence can be effectively quenched by Au@AgNPs via fluorescence resonance energy transfer (FRET) or inner filter effect (IFE). To further verify the fluorescence quenching effect of Au@AgNPs on CQDs, the fluorescence spectra of CQDs in different systems were measured. As depicted in Fig.S2, the fluorescence spectra of CQDs and CQDs-EA mixture almost overlaps, indicating that EA has no effect on the fluorescence emission of CQDs. When the CQDs were mixed with AuNPs, $AgNO_3$, AuNPs-$AgNO_3$ and EA-$AgNO_3$ respectively, their fluorescence decreased slightly. However, the fluorescence of CQDs decreased dramatically when mixed with AuNPs-$AgNO_3$-EA. As noted, EA can reduce Ag^+ to Ag which deposit on the surfaces of AuNPs to form Au@AgNPs. Thus, the significant quenching of CQDs fluorescence can be attributed to the formation of Au@AgNPs. The fluorescence quenching mechanism includes FRET, IFE, static quenching, dynamic quenching, and so on. One of the conditions for FRET is that the distance between donor and receptor is close enough, typically within 10 nm. The zeta potentials of CQDs and Au@AgNPs in BR buffer (pH 8.5) were measured to be −31.96 mV and −14.36 mV (Fig. S3.), respectively, proposing that the distance between CQDs and Au@AgNPs is too large to meet the condition of FRET due to the electrostatic repulsion between them [47]. Considering that the absorption spectra of Au@AgNPs overlaps with both excitation and emission spectra of CQDs (Fig.3B), we believe that the significant decrease in CQDs fluorescence is caused by the IFE of Au@AgNPs. The fluorescence intensity values at 405 nm of CQDs- AuNPs- $AgNO_3$ system after the addition of EA with different concentrations were recorded, and the dependence of F_0/F on EA concentration was displayed in Fig. S4. Although the fluorescence intensity ratio increases with the increase of EA concentration, it does not conform to the traditional linear Stern-Volmer equation [48, 49]. The up-curving Stern-Volmer plot reveals that

both dynamic and static quenching processes take place in this system.

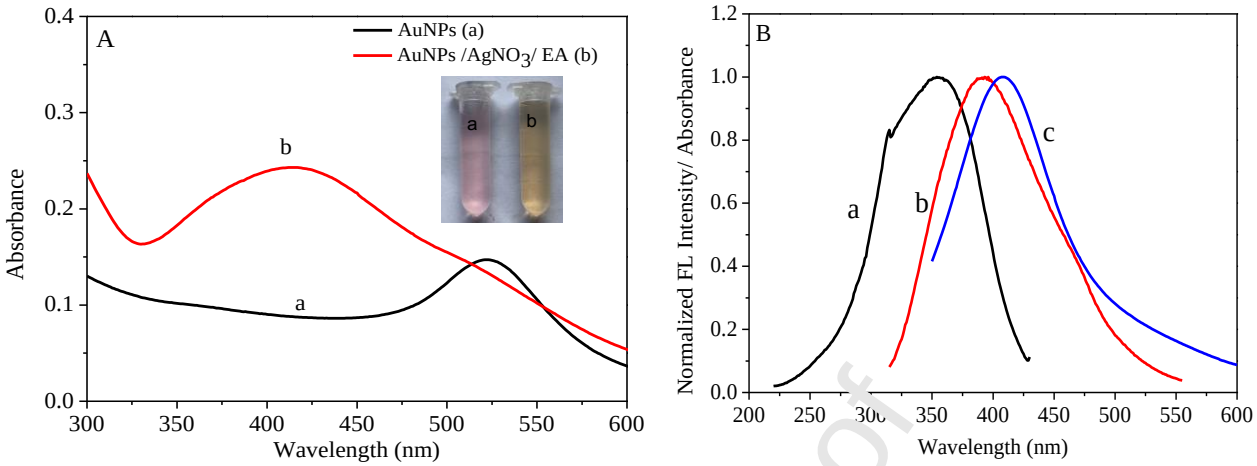

Fig.3. (A) Absorption spectra and photographs of AuNPs and AuNPs-$AgNO_3$-EA system (AuNPs: 0.5 nM; $AgNO_3$: 200 μM; EA: 2.5μM); (B) Normalized (a) excitation, (b) emission spectra of CQDs and (c) absorption spectra of Au@AgNPs.

With the introduction of EA into CQDs-AuNPs-$AgNO_3$ system, CQDs fluorescence is effectively quenched, and the degree of quenching increases with the increase of EA concentration (Fig.4A). As observed in Fig. 4B, a new absorption peak at 413 nm appears with the introduction of EA, furthermore, the absorbance increases with the increase of EA concentration. Therefore, by monitoring CQDs fluorescence at 405 nm and Au@AgNPs absorbance at 413 nm, a double signal method for assaying of EA can be established.

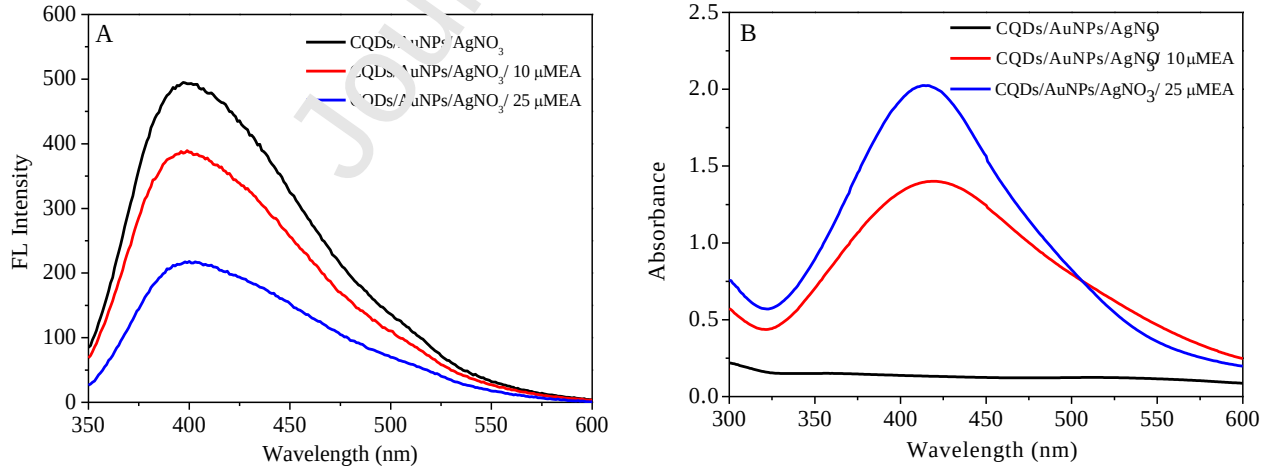

Fig.4. (A) Fluorescence emission spectra and (B) absorption spectra of CQDs-AuNPs-$AgNO_3$ system at different EA concentrations.

3.4 Optimization of determination conditions

In order to get the best signal response from the CQDs-AuNPs-$AgNO_3$ system, three factors,

Ag^+ ions concentration, pH value of buffer and reaction time, which may affect the change of fluorescence and absorbance, were investigated using fluorescence as an example and ΔF as criterion.

As the key factor for quenching of CQDs fluorescence and resulting in UV-response, the Ag^+ ions concentration plays an important role in improving the analytical performance of the method. First, the $AgNO_3$ concentration ranging from 50 to 400 μM for the formation of Au@AgNPs were optimized. As noticed in Fig.S5A, with the increase of Ag^+ ions concentration, the ΔF value increases rapidly. Whereas the Ag^+ ions concentration exceeds 200 μM, the ΔF value remains unchanged. Thus, 200 μM $AgNO_3$ was chosen for the further experiments. Under alkaline condition, the electron cloud density on benzene ring increases due to the ionization of phenolic hydroxyl groups in EA molecule. The research demonstrated that alkaline environment was favorable to the reduction of Ag^+ ions by EA and the deposition of Ag atoms on the surface of AuNPs [35]. Second, the effect of pH on ΔF was studied by using BR buffer with pH value in the range of 7.0 to 10.5. It is found that the ΔF reaches the maximum at pH 8.5, and beyond this pH, ΔF begins to slowly decrease (Fig. S5B). Hence, pH 8.5 was chosen as an optimized condition. Third, at room temperature, the influence of different reaction time (2~20 min) on ΔF was also investigated (Fig. S5C). The reaction can reach equilibrium within 6 min. If the reaction time continues to be prolonged, the ΔF value will decrease. In this study, 6 min was selected as the best reaction time.

3.5 Detection of EA based on fluorescence and UV-vis

Under the optimum conditions, the influence of EA concentration on the fluorescence and absorption spectra of CQDs-AuNPs-$AgNO_3$ system were studied. As presented in Fig. 5A, the fluorescence emission intensity of CQDs at 405 nm decreases gradually with increasing EA concentration from 0.50 to 40.0 μM. Under 365 nm UV lamp, the blue fluorescence of the corresponding solution decreases in turn (Fig. 5A inset). Linear fitting shows that the decrease of fluorescence (ΔF) was linear to EA concentration in the range of 0.50-25.0 μM (Fig. 5B) with a regression equation $\Delta F = 10.748C + 3.524$ and $R^2 = 0.996$. The limit of detection (LOD) based on 3σ/k for ten blank determinations was 0.41μM. As seen in Fig. 5C, the absorbance at 413 nm enhances with the increase of EA concentration. Inset in Fig. 5C is the digital picture of CQDs-AuNPs-$AgNO_3$ system in the presence of EA of various concentrations, indicating that the color change induced by EA is significant. The plot of ΔA against the concentration of EA exhibits

an excellent linear response from 0.50 to 25.0 μM (Fig. 5D). The linear regression equation could be described as $\Delta A = 0.076C + 0.080$ with a correlation coefficient (R^2) of 0.997. The LOD was as low as 0.22μM (3σ/k, n=10), showing high sensitivity for EA assay. All of these results confirm that CQDs-AuNPs-$AgNO_3$ system with two different signals could be applied in detection of EA.

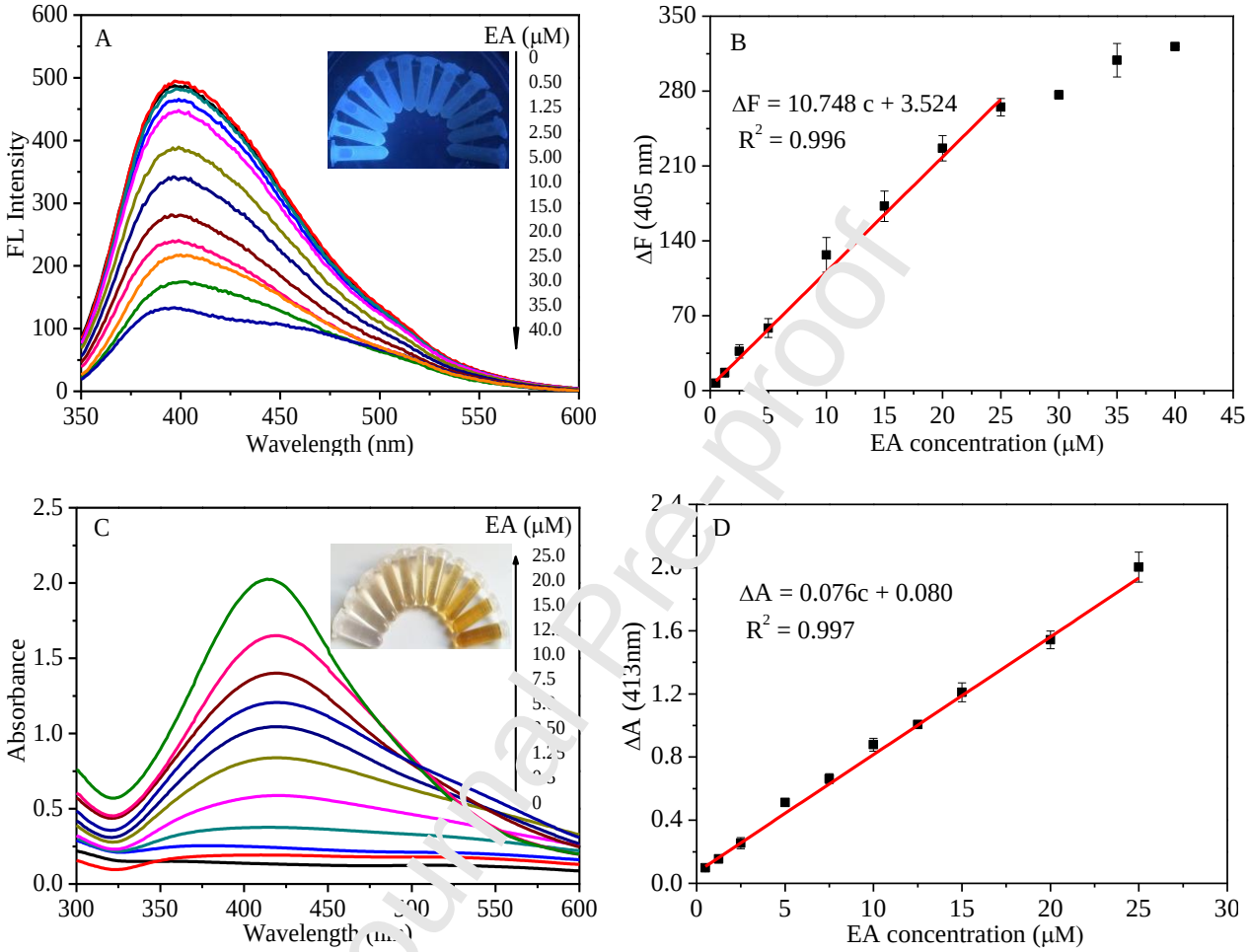

Fig.5. (A) The fluorescence spectra and photographs (under UV lamp) of CQDs-AuNPs-$AgNO_3$ system in the presence of different concentrations of EA. (B) The linear relationship between ΔF and EA concentration (n=3). (C) UV-vis absorption spectra and photographs of CQDs-AuNPs-$AgNO_3$ in the presence of different concentrations of EA. (D) The linear relationship between ΔA and EA concentration (n=3). Experimental conditions: $AgNO_3$, 200 μM; AuNPs, 0.05 nM; pH 8.5; reaction time, 6 min.

A comparison between our method with other reported methods for EA determination is summarized in Table 1. The established method is superior to most of the approaches for EA analysis in linear range and response time. Although the LOD obtained by our method is not the lowest, the probes used in this study are composed of CQDs and Au@AgNPs grown in situ, which can be prepared under simple conditions, and the introduction of EA can generate a double signal response. Compared with the single signal sensing, the double signal sensing based on fluorescence

and UV-vis can make the detection results more reliable.

Table 1 Comparison of different methods for EA detection

Method	Linear range (μM)	LOD (μM)	Analysis time	References
Resonance light scattering	0.2-20.0	0.04	20	[35]
Resonance light scattering	0.053-13.2	0.046	6.0	[36]
Fluorimetry	1.03-182	0.31	20	[40]
HPLC-DAD	1.65-33.0	-	3.8	[50]
HPLC-DAD	1.66-182	0.33	15	[51]
UV spectrometry	1.65-26.5	0.66	-	[43]
Capillary Electrophoresis	131.8-1054	7.20	12.2	[38]
Voltammetric	0.1-1.50	0.01	-	[31]
Colorimetry	0.5-25.0	0.22	6.0	This work
Fluorimetry	0.5-25.0	0.41	6.0	This work

3.6 Selectivity towards EA detection

In order to evaluate the selectivity of the double signal probe, the fluorescence and colorimetric response of CQDs-AuNPs-$AgNO_3$ system to other common substances in commercial skin-whitening cosmetics were investigated according to the procedure described in section 2.3. Fig. 6A and B show the ΔF and ΔA values of EA alone or coexisting with other interferences in the system, respectively. Although the interference concentration is five or ten times higher than that of EA, no obvious changes in ΔF and ΔA values are found, suggesting a high selectivity toward EA. Thus, this method does not need tedious sample processing and is suitable for EA detection in complex samples.

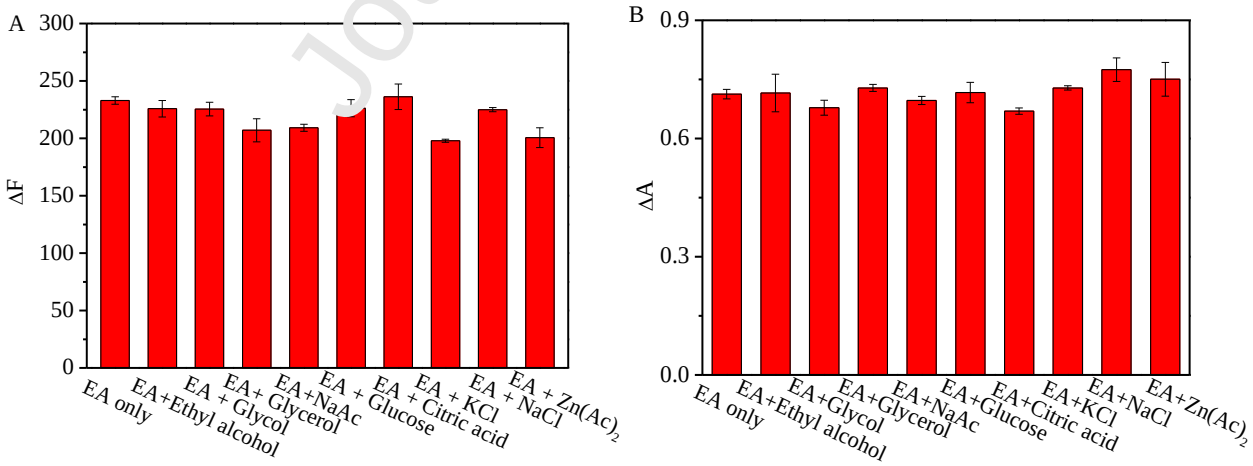

Fig.6. The ΔF and ΔA of CQDs-$AuNP_S$-$AgNO_3$ in the presence of EA and other common substances. The EA concentration was 20 μM, the concentrations of ethylalcohol, glycol, glycerol, NaAc, glucose in the solution was 200μM, respectively, and citric acid, KCl, NaCl, $Zn(Ac)_2$ in the solution was 100μM, respectively.

3.7. Detection of EA in real samples

In order to verify the feasibility of the method, it was employed to detect EA in ellagic acid serum samples purchased from a local supermarket. Two samples were prepared and three parallel experiments were carried out on each sample. The results are given in Table 2, the content of EA determined by fluorescence are consistent with those by colorimetric method. Furthermore, the spiked recoveries experiments were carried out and the recoveries are between 94.8% and 112% with relative standard deviations (RSD) less than 5.0 %. These results demonstrate that the method has acceptable reliability and good repeatability in practical sample analysis.

Table 2 The determination results of EA in commercial cosmetics

		Fluorometric method			Colorimetric method		
Samples	Added(μM)	Found (μM)	Recovery (%)	RSD (n=3,%)	Found (μM)	Recovery (%)	RSD (n=3,%)
	0	1.71		0.6	1.64		1.8
sample 1	2	3.95	112	1.7	3.78	107	1.2
	5	7.04	107	3.8	7.08	108	2.2
	0	2.03		2.5	2.05		1.7
sample 2	2	4.03	100	1.8	4.10	102	4.0
	5	6.77	94.8	2.2	7.09	101	0.9

4. Conclusions

In this work, CQDs with QYs of 23% were prepared from trifolium leaves by simple hydrothermal method. A double signal probe composed of CQDs and Au@AgNPs grown in situ was designed for EA determination by fluorescence and colorimetric methods. The detection principle was illustrated by using different analysis techniques such as TEM images, fluorescence spectra, UV-vis spectra, and zeta potential measurements. Good linear relationship between signal response and EA concentration within 0.50-25.0 μM were achieved, and low detection limit of 0.41 μM (fluorescence) and 0.22 μM (colorimetric) were obtained. More importantly, the designed probe was successfully applied for the detection of EA in cosmetics samples with satisfactory results, demonstrating the potential of the probe in practical applications. Although the analytical method has some shortcomings, for example, time-consuming preparation of nanomaterials, inappropriate for continuous and in vivo analysis, CQDs as fluorescence probe shows several advantages over organic fluorescent dyes and semiconductor quantum dots, including sufficient carbon sources, easy preparation, no toxicity and strong fluorescence emission. On the other hand, compared with other methods, colorimetry with Au@AgNPs as chromophores has the advantages of high sensitivity, no

need of expensive equipment, simple operation, etc.

Declaration of competing interest

The authors declare that they have no competing interests.

Acknowledgements

The present work was supported by the National Natural Science Foundation of China (61664002) and the Innovation Project of Guangxi Graduate Education (YCSW2020016).

References

[1] Yola M L, Electrochemical activity enhancement of monodisperse boron nitride quantum dots on graphene oxide: Its application for simultaneous detection of organophosphate pesticides in real samples. J. Mol. Liq. 277 (2019) 50-57. https://doi.org/10.1016/j.molliq.2018.12.084

[2] Liu H, Sun Y, Li Z, Yang R, Yang J, Aryee A A, Zhang X, Ge J, Qu L, Lin Y SciFinder-guided rational design of fluorescent carbon dots for ratiometric monitoring intracellular pH fluctuations under heat shock. Chin. Chem. Lett. 30 (2019) 1647-1651. https://doi.org/10.1016/j.cclet.2019.06.012

[3] Carnerero J M, Sánchez-Coronilla A, Jimenez-Ruiz A, Prado-Gotor R, Factors that control the gold nanoparticles' aggregation induced by adenine molecules: New insights through a combined experimental and theoretical study. J. Mol. Liq. 310 (2020) 113136. https://doi.org/10.1016/j.molliq.2020.113136

[4] Rao H, Xue X, Wang H, Xue Z, Gold nanorod etching-based multicolorimetric sensors: strategies and applications. Journal of Materials Chemistry C 7 (2019) 4610-4621 https://doi.org/10.1039/C9TC00757A

[5] Chen N, Liu H, Zhang Y, Zhou Z, Fan W, Yu G, Shen Z, Wu A, A colorimetric sensor based on citrate-stabilized AuNPs for rapid pesticide residue detection of terbuthylazine and dimethoate. Sens and Actuators B: Chem 255(2018)3093-3101 https://doi.org/10.1016/j.snb.2017.09.134

[6] Modrzejewska-Sikorska A, Konował E, Silver and gold nanoparticles as chemical probes of the presence of heavy metal ions. J. Mol. Liq. 302 (2020) 112559. https://doi.org/10.1016/j.molliq.2020.112559

[7] Zeng J, Fan S, Zhao C, Wang Q, Zhou T, Chen X, Yan Z, Li Y, Xing W, Wang X, A

colorimetric agarose gel for formaldehyde measurement based on nanotechnology involving Tollens reaction. Chem Commun (Camb) 50 (2014) 8121-8123 https://doi.org/10.1039/C4CC00914B

[8] Zong C, Li B, Wang J, Liu X, Zhao W, Zhang Q, Nie X, Yu Y, Visual and colorimetric determination of H2O2 and glucose based on citrate-promoted H2O2 sculpturing of silver nanoparticles. Microchim Acta 185 (2018)199 https://doi.org/10.1007/s00604-018-2737-2

[9] Xiong Y, Zhang Y, Rong P, Yang J, Wang W, Liu D, A high-throughput colorimetric assay for glucose detection based on glucose oxidase-catalyzed enlargement of gold nanoparticles. Nanoscale 7 (38) (2015)15584-15588 https://doi.org/10.1039/C5NR03758A

[10] Gao J, Jia M, Xu Y, Zheng J, Shao N, Zhao M, Prereduction-promoted enhanced growth of silver nanoparticles for ultrasensitive colorimetric detection of alkaline phosphatase and carbohydrate antigen 125. Talanta 189(2018)129-136 https://doi.org/10.1016/j.talanta.2018.06.064

[11] Virel A, Saa L , Pavlov V, Modulated Growth of Nanoparticles. Application for Sensing Nerve Gases. Anal Chem 81(2009) 268-272. https://doi.org/10.1021/ac801949x

[12] Liu H, Sun Y, Yang J, Hu Y, Yang R, Li Z, Qu L, Lin Y, High performance fluorescence biosensing of cysteine in human serum with superior specificity based on carbon dots and cobalt-derived recognition. Sens and Actuators B: Chem 28 (2019) 62-68 https://doi.org/10.1016/j.snb.2018.10.029

[13] Su A, Zhong Q, Chen Y, Wang Y. Preparation of carbon quantum dots from cigarette filters and its application for fluorescence detection of Sudan I. Anal Chim Acta 1023 (2018) 115-120 https://doi.org/10.1016/j.aca.2018.03.024

[14] Geng X, Sun Y, Guo Y, Zhao Y, Zhang K, Xiao L, Qu L, Li Z Fluorescent Carbon Dots for in Situ Monitoring of Lysosomal ATP Levels. Anal Chem 92 (2020) 7940-7946. https://doi.org/10.1021/acs.analchem.0c01335

[15] Lu M, Duan Y, Song Y, Tan J, Zhou L, Green preparation of versatile nitrogen-doped carbon quantum dots from watermelon juice for cell imaging, detection of Fe3+ ions and cysteine, and optical thermometry. J. Mol.Liq. 269 (2018) 766-774. https://doi.org/10.1016/j.molliq.2018.08.101

[16] Liu H, Yang J, Li Z, Xiao L, Aryee AA, Sun Y, Yang R, Meng H, Qu L, Lin Y, Zhang X, Hydrogen-Bond-Induced Emission of Carbon Dots for Wash-Free Nucleus Imaging. Anal Chem 91 (2019) 9259-9265 https://doi.org/10.1021/acs.analchem.9b02147

[17] Zhong Q, Chen Y, Su A, Wang Y, Synthesis of catalytically active carbon quantum dots and its

application for colorimetric detection of glutathione. Sens and Actuators B: Chem 273(2018) 1098-1102 https://doi.org/10.1016/j.snb.2018.07.026

[18] Yuan C , Qin X, Xu Y, Li X, Chen Y, Wang Y, Carbon quantum dots originated from chicken blood as peroxidase mimics for colorimetric detection of biothiols. Journal of Photochemistry & Photobiology A: Chemistry 396 (2020)112529 https://doi.org/10.1016/j.jphotochem.2020.112529

[19] Chandra S, Singh VK, Yadav PK, Bano D, Kumar V, Pandey VK, Talat M, Hasan SH, Mustard seeds derived fluorescent carbon quantum dots and their peroxidase-like activity for colorimetric detection of H2O2 and ascorbic acid in a real sample. Anal Chim Acta 1054 (2019) 145-156. https://doi.org/10.1016/j.aca.2018.12.024

[20] Zhong Q, Chen Y, Qin X, Wang Y, Yuan C, Xu Y, Colorimetric enzymatic determination of glucose based on etching of gold nanorods by iodine and using carbon quantum dots as peroxidase mimics. Microchim Acta 186 (2019) 161. https://doi.org/10.1007/s00604-019-3291-2

[21] Dai H, Shi Y, Wang Y, Sun Y, Hu J, Ni P, Li Z, A carbon dot based biosensor for melamine detection by fluorescence resonance energy transfer. Sens and Actuators B: Chem 202 (2014) 201-208 https://doi.org/10.1016/j.snb.2014.05.068

[22] Chen Y, Qin X, Yuan C, Wang Y, Switch on fluorescence mode for determination of l-cysteine with carbon quantum dots and Au nanoparticles as a probe. RSC Adv 10 (2020) 1989-1994. https://doi.org/10.1039/C9RA09019C

[23] Yang Y, Huo D, Wu H, Wang X, Yang J, Bian M, Ma Y, Hou C, N, P-doped carbon quantum dots as a fluorescent sensing platform for carbendazim detection based on fluorescence resonance energy transfer. Sens and Actuators B: Chem 274 (2018) 296-303. https://doi.org/10.1016/j.snb.2018.07.130

[24] Liu W, Ding F, Wang Y, Mao L, Liang R, Zou P, Wang X, Zhao Q, Rao H, Fluorometric and colorimetric sensor array for discrimination of glucose using enzymatic-triggered dual-signal system consisting of Au@Ag nanoparticles and carbon nanodots. Sens and Actuators B: Chem 265 (2018) 310-317 https://doi.org/10.1016/j.snb.2018.03.060

[25] Chen C, Zhang G, Ni P, Jiang Y, Lu Y, Lu Z, Fluorometric and colorimetric dual-readout alkaline phosphatase activity assay based on enzymatically induced formation of colored Au@Ag nanoparticles and an inner filter effect. Microchim Acta 186 (2019) 348 https://doi.org/10.1007/s00604-019-3478-6

[26] Shi Y, Pan Y, Zhang H, Zhang Z, Li MJ, Yi C, Yang M, A dual-mode nanosensor based on carbon quantum dots and gold nanoparticles for discriminative detection of glutathione in human plasma. Biosens Bioelectron 56(2014)39-45 https://doi.org/10.1016/j.bios.2013.12.038

[27] Zhao D, Chen C, Sun J, Yang X, Carbon dots-assisted colorimetric and fluorometric dual-mode protocol for acetylcholinesterase activity and inhibitors screening based on the inner filter effect of silver nanoparticles. Analyst 141 (2016) 3280-3288 https://doi.org/10.1039/C6AN00514D

[28] Wu X, Song Y, Yan X, Zhu C, Ma Y, Du D, Lin Y, Carbon quantum dots as fluorescence resonance energy transfer sensors for organophosphate pesticides determination. Biosens Bioelectron 94 (2017) 292-297. https://doi.org/10.1016/j.bios.2017.03.010

[29] Chen Y, Qin X, Yuan C, Shi R, Wang Y, Double responsive analysis of carbaryl pesticide based on carbon quantum dots and Au nanoparticles. Dyes and Pigments 181(2020) 108529 https://doi.org/10.1016/j.dyepig.2020.108529

[30] Zhang L, Liu Y, Hu X, Xu M, Wang Y, Studies on interactions of pentagalloyl glucose, ellagic acid and gallic acid with bovine serum albumin: A spectroscopic analysis. Food Chem 324(2020) https://doi.org/10.1016/j.foodchem.2020.12[illegible]872

[31] Cuartero M, Ortuño JA, Truchado P, García MS, Tomás-Barberán FA, Albero MI ,Voltammetric behaviour and square-wave voltammetric determination of the potent antioxidant and anticarcinogenic agent ellagic acid in foodstuffs. Food Chem 128 (2011) 549-554. https://doi.org/10.1016/j.foodchem.2011.03.064

[32] Tokutomi H, Takeda T, Hoshino N, Akutagawa T, Molecular Structure of the Photo-Oxidation Product of Ellagic Acid in Solution. ACS Omega 3 (9) (2018) 11179-11183. https://doi.org/10.1021/acsomega.8b01716

[33] Hsu CC, Chao YY, Wang SW, Chen YL, Polyethylenimine-capped silver nanoclusters as fluorescent sensors for the rapid detection of ellagic acid in cosmetics. Talanta 204 (2019)484-490. https://doi.org/10.1016/j.talanta.2019.06.047

[34] Bala I , Bhardwaj V , Hariharan S,Analytical methods for assay of ellagic acid and its solubility studies. journal of pharmaceutical & biomedical analysis 40(2006)206-210.https://doi.org/10.1016/j.jpba.2005.07.006

[35] Wang Y, Zeng Y, Fu W, Zhang P, Li L, Ye C, Yu L, Zhu X, Zhao S,Seed-mediated growth of Au@Ag core-shell nanorods for the detection of ellagic acid in whitening cosmetics. Anal Chim

Acta 1002(2018) 97-104. https://doi.org/10.1016/j.aca.2017.11.067

[36] Chen Z, Peng Y, Wang S, Chen X, Song T, Qian S, Chen M, Wang Q, Use of Gemini surfactant in a one-step ellagic acid assay by resonance light scattering technique. Talanta 82 (2010) 885-891. https://doi.org/10.1016/j.talanta.2010.04.032

[37] Amakura Y , Okada M , Tsuji S, High-performance liquid chromatographic determination with photodiode array detection of ellagic acid in fresh and processed fruits. Journal of Chromatography A 896 (2000) 87-93. https://doi.org/10.1016/S0021-9673(00)00414-3

[38] Zhou B, Wu Z, Li X, Zhang J, Hu X, Analysis of ellagic acid in pomegranate rinds by capillary electrophoresis and high-performance liquid chromatography. Phytochem Anal 19 (2008)86-89.https://doi.org/10.1002/pca.1054

[39] Sadecka J, Tothova J, Spectrofluorimetric determination of ellagic acid in brandy. Food Chem 135 (2012) 893-897. https://doi.org/10.1016/j.foodchem.2012.06.019

[40] Shen Y, Liu S, Wang J, Li D, Determination of ellagic acid by fluorescence quenching method with glutathione capped CdTe quantum dots as the probe. Analytical Methods 5(2013)3228. https://doi.org/10.1039/C3AY40365C

[41] Bala R, Sharma RK, Wangoo N, Highly sensitive colorimetric detection of ethyl parathion using gold nanoprobes. Sens and Actuators B: Chem 210 (2015) 425-430. https://doi.org/10.1016/j.snb.2014.12.123

[42] Ma J-L, Yin B-C, Wu X, Ye B-C, Simple and Cost-Effective Glucose Detection Based on Carbon Nanodots Supported on Silver Nanoparticles. Anal Chem 89 (2016) 1323-1328. https://doi.org/10.1021/acs.analchem.6b04259

[43] Liu J, Wang L, Bao H, A novel fluorescent probe for ascorbic acid based on seed-mediated growth of silver nanoparticles quenching of carbon dots fluorescence. Anal Bioanal Chem 411 (2019) 877-883. https://doi.org/10.1007/s00216-018-1505-9

[44] Kumar A , Chowdhuri A R , Laha D, Green synthesis of carbon dots from Ocimum sanctum for effective fluorescent sensing of Pb2+ ions and live cell imaging[J]. Sens and Actuators B: Chem 242 (2016)679–686.https://doi.org/10.1016/j.snb.2016.11.109

[45] Singh S, Vaishnav JK, Mukherjee TK, Quantum Dot-Based Hybrid Coacervate Nanodroplets for Ultrasensitive Detection of Hg2+. ACS Applied Nano Materials 3 (2020)3604-3612 https://doi.org/10.1021/acsanm.0c00317

[46] Rosenau T, Potthast A, Adorjan I, Hofinger A, Sixta H, Firgo H, Kosma P, Cellulose solutions inN-methylmorpholine-N-oxide (NMMO)–degradation processes and stabilizers. Cellulose 9 (2002) 283-291 http://doi.org/10.1023/a:1021127423041

[47] Chen C, Zhao D, Sun J, Yang X, A dual-mode signaling response of a AuNP-fluorescein based probe for specific detection of thiourea. Analyst 141 (2016) 2581-2587 https://doi.org/10.1039/C6AN00165C

[48] Luo B, Yang H, Zhou B, Ahmed SM, Zhang Y, Liu H, Liu X, He Y, Xia S, Facile Synthesis of Luffa Sponge Activated Carbon Fiber Based Carbon Quantum Dots with Green Fluorescence and Their Application in Cr(VI) Determination. ACS Omega 5 (2020) 5540-5547. https://doi.org/10.1021/acsomega.0c00195

[49] Liu S, Tian J, Wang L, Zhang Y, Qin X, Luo Y, Asiri AM, Al-Youbi AO, Sun X, Hydrothermal treatment of grass: a low-cost, green route to nitrogen-doped, carbon-rich, photoluminescent polymer nanodots as an effective fluorescent sensing platform for label-free detection of Cu(II) ions. Adv Mater 24 (2012) 2037-2041 https://doi.org/10.1002/adma.201200164

[50] Ratnam D V , Bhardwaj V , Kumar M, Simultaneous analysis of ellagic acid and coenzyme Q10 by derivative spectroscopy and HPLC. Talanta 70 (2006) 387-391. https://doi.org/10.1016/j.talanta.2006.02.057

[51] Zehl M, Braunberger C, Conrad J, Crnogorac M, Krasteva S, Vogler B, Beifuss U, Krenn L, Identification and quantification of flavonoids and ellagic acid derivatives in therapeutically important Drosera species by LC-DAD, LC-NMR, NMR, and LC-MS. Anal Bioanal Chem 400 (2011) 2565-2576 http://dx.doi.org/10.1007/s00216-011-4690-3

Author statement

The work described has not been published before; it is not under consideration for publication anywhere else; and publication has been approved by all co-authors and the responsible authorities at the institute(s) where the work has been carried out; if accepted, it will not be published elsewhere in the same form, in English or in any other language, including electronically without the written consent of the copyright-holder.

Dr. Yilin Wang

Declaration of interests

☑ The authors declare that they have no known competing financial interests or personal relationships that could have appeared to influence the work reported in this paper.

☒ The authors declare the following financial interests/personal relationships which may be considered as potential competing interests:

Research Highlights

- A colorimetric and fluorescent double reading method for ellagic acid determination was established.
- The proposed method was successfully applied to the detection of ellagic acid in real samples.
- The advantages of the method are simplicity, high accuracy and good precision.